engineering proceedings

MDPI

*Proceeding Paper*

# DFKI-X2D: Design and Testing of a Quasi-Direct Drive Motor for Space Applications †

**Jonas Eisenmenger *, Zhongqian Zhao, Pierre Willenbrock and Wiebke Brinkmann**

German Research Center for Artificial Intelligence (DFKI) GmbH, 28359 Bremen, Germany; zhongqian.zhao@dfki.de (Z.Z.); pierre.willenbrock@dfki.de (P.W.); wiebke.brinkmann@dfki.de (W.B.)

* Correspondence: jonas.eisenmenger@dfki.de; Tel.: +49-421-17845-4151

† Presented at the 15th EASN International Conference, Madrid, Spain, 14–17 October 2025.

**Abstract**

Due to the high level of innovation involved, and the requirements arising from a new environment, the use of a quasi-direct drive motor for space applications presents not only several challenges, but also great opportunities. Such a motor is particularly well-suited to dynamic applications like walking robots or robotic arms. To ensure that it can withstand the environmental challenges, the motor must undergo extensive testing. This paper briefly outlines the development of such a motor based on prior prototypes with different design concepts. It addresses the specific requirements of a space variant and describes the selected final design. Additionally, the development of corresponding motor electronics is described. Finally, the results of a test campaign are presented. The campaign included internal functional tests to characterize the motor and external environmental tests necessary for space qualification. These tests included vibration, thermal vacuum chamber (TVAC) and electromagnetic compatibility (EMC) tests. Together, they showcased a highly dynamic motor with an efficiency of up to 90% and moved it towards a technology readiness level (TRL) of 5.

**Keywords:** robotics; quasi-direct drive; space technology; walking robots; TRL

## 1. Introduction

Robotic systems are increasingly being developed for exploration of extraterrestrial areas such as the Moon, Mars, asteroids, and other celestial bodies. Due to the impact of space debris in orbit, current developments are focused on sustainability and recyclability. Modular approaches are being pursued in this regard. In this context, developments for planetary missions are also being designed with sustainability and modularity in mind. The MODKOM project (Modular components as Building Blocks for application-specific configurable space robots) adopted a modular approach and successfully developed several modular components and modules [1]. One such component is the German Research Center for Artificial Intelligence (DFKI) X2D joint, a quasi-direct drive motor for space applications [2].

Direct or quasi-direct drive motors are particularly suitable for use in walking robots due to their high dynamic movement capability. While there are already terrestrial applications (e.g., MIT's Mini Cheetah [3], and Unitree's A1 [4]), there are none yet in extraterrestrial applications. Dynamic walking robots with quasi-direct drive motors would have the potential to reach locations with difficult terrain where rovers would still fail [5,6]. However, conventional quasi-direct drive motors cannot be used in space as they are not

Check for updates

Academic Editors: Spiros Pantelakis, Andreas Strohmayer and Gustavo Alonso

Published: 21 April 2026

**Copyright:** © 2026 by the authors. Licensee MDPI, Basel, Switzerland. This article is an open access article distributed under the terms and conditions of the Creative Commons Attribution (CC BY) license.

designed for extreme environmental conditions such as those on the Moon, and factors such as thermal design must be considered [7].

The DFKI-X2D was developed as an attempt to find a compromise between high mass-specific torque, impact mitigation, and motor efficiency, resulting in a quasi-direct drive design that is suitable for space applications. Two prototypes were therefore developed, comparing in-runner and out-runner approaches involving different gear ratios, to find the optimal combination that would minimize power losses and ensure good thermal behavior while maintaining dynamic properties [2]. Following testing of the prototypes, the DFKI-X2D was further developed into a space version, for which associated motor electronics were also established. Both underwent initial functional tests, followed by environmental tests such as vibration tests, thermal vacuum chamber (TVAC) tests, and electromagnetic compatibility (EMC) tests, to validate the designs. The paper describes the further development of the DFKI-X2D joint and its motor electronics, as well as the results of testing and possible applications.

## 2. DFKI-X2D Design

Based on previously developed prototypes and the results of their testing [2], a final space iteration of the motor and electronics was designed. New space-relevant requirements were therefore selected to create a design that could undergo qualification testing and reach a high technology readiness level (TRL). This section gives a short overview of the further-developed DFKI-X2D; more detailed information on the requirements and mechanical design can be found in [2].

### *2.1. Requirements*

To determine the requirements, an example of a possible mission for a dynamic walking robot on the Moon was selected. Therefore, a temperature range of −40 °C to 120 °C was chosen, representing approximately ten days on the lunar surface [8]. During lunar night, the robot would require protection and heating. Simulations of a 40 kg walking robot under moon gravity, with the addition of a safety factor, resulted in the selection of a nominal torque of 8 Nm, a peak torque of 30 Nm and a maximum velocity of 200 rpm.

### *2.2. Mechanics*

The design of the DFKI-X2D is closely based on the in-runner prototype [2]. It uses the same Robodrive ILM-85x23 in-runner motor, as the prototype's performance and thermal behavior were already very good. The bearing design continued to incorporate a soft preloaded back-to-back approach at the rotor and output sites. The bearings were replaced with space-graded versions. The major changes compared to the prototype were the selection of a one-stage planetary gearbox with a 7:1 reduction for greater efficiency and back-drivability, and the addition of connectors for power and data transfer to provide EMC protection. The DFKI-X2D has a diameter of 92 mm (max. 108 mm at the flange) and a length of 98 mm, weighing 1.5 kg. All parts were selected as space-graded versions for the entire design, and gold-anodized aluminum was used to avoid cold welding and improve thermal behavior [9]. A cross-section of the motor and a photograph of the assembled version are shown in Figure 1.

https://doi.org/10.3390/engproc2026133027

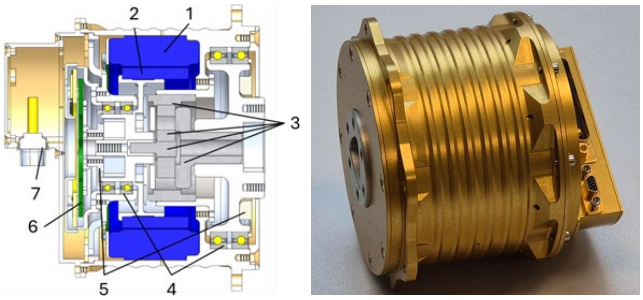



**Figure 1.** Cross-section view of DFKI-X2D and assembled version. 1: Stator. 2: Rotor. 3: Planetary gearbox components. 4: Angular bearings. 5: Diaphragm spring. 6: Encoder. 7: Connector.

### *2.3. Electronics*

The motor electronics which control the motor were developed in two iterations. The initial iteration was designed as a breadboard to test the design. The subsequent iteration was developed as a space version, which will be outlined in this section.

The electronics were designed with a 50 VDC bus voltage and a peak phase current capability of 30 A. The layout can be divided into three different segments: The power section has an input for the power source and an output for the Pulse Width Modulation (PWM) signal. The microcontroller section includes interfaces for communication and sensors. The bulk section containing filters and capacitors to improve EMC, among other things. These segments are distributed on a rigid–flex circuit board to avoid the use of plug connections. These were used in the first iteration as a stacked design. It is populated on only one side; this not only simplifies manufacturing but also improves thermal management under vacuum conditions. The circuit board design and layout, as well as the derating of component parameters, were implemented in accordance with European Cooperation for Space Standardization (ECSS) regulations. Component selection focused on higher-quality components with direct equivalents at aerospace-quality levels. In addition, a housing for the electronics was designed. This consisted of three parts: the body, a cover, and a center piece. The center piece was used to attach the folded flex circuit board. The center piece and circuit board were then screwed to the body. To transfer heat from the circuit board to the housing as efficiently as possible, a low-outgassing GTS8-85 thermal pad from Getelec SAS (Buc, France) was placed between the circuit board and the body. Two D-SUB DB-5W5 connectors (male and female), four 9-position Micro-D connectors and three 9-position D-SUB connectors were also provided to support the electronics' various functions. These were selected in accordance with ECSS standards and procured as EMC-protected, space-qualified variants. The design of the electronics is shown in Figure 2.

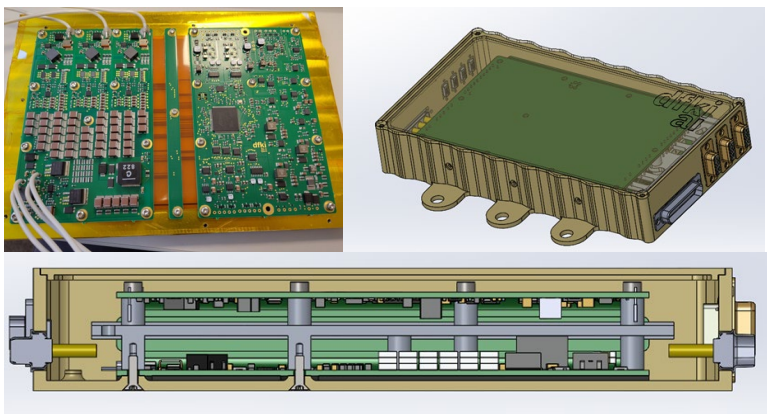


**Figure 2.** (**top left**): flex circuit board; (**top right**): assembled design; (**bottom**): cross-section view.

https://doi.org/10.3390/engproc2026133027

## 3. Testing

Multiple tests were conducted to validate the designs and to determine the motor characteristics. These were divided into internal functional tests, such as starting up the motor with the electronics and characterizing it on a motor test bench, and external qualification tests, including vibration, TVAC, and EMC tests.

### 3.1. Motor Characterization

A motor test bench was used to characterize the motor, with the DFKI-X2D connected to an electrical brake with a torque sensor in between. First, the motor was tested with a commercial motor controller to identify its best-case characteristic values. Thereafter, it was tested with the developed electronics for comparison. No-load and load tests were performed to determine the current-to-torque and speed-to-torque ratios, as well as the motor's efficiency. These values were used to generate a typical motor characteristic curve. Additionally, efficiency at different speeds and torques was determined by testing a range of velocities at different set torques, creating an efficiency heat map. Backdrivability was measured to enable comparison of the new design with the prototype.

### 3.2. Vibration Tests

The vibration tests were performed in accordance with ECSS standards (ECSS-E-HB-32-26A [10]) at ZARM Technik AG, as was done for the prototypes [2]. For sine vibrations, the recommended qualification loads for masses under 100 kg were used [10] (p. 203); for random vibration tests, the loads were determined using the masses of the DFKI-X2D and electronics [10] (p. 240). To validate the performance of the motor and electronics, they were tested together before and after each vibration run (resonance search, sine vibrations and random vibrations) along the three different axes. This involved giving a velocity command and measuring the current consumption under no-load. This allowed possible changes and the general functionality of both to be tested.

### 3.3. TVAC Tests

The TVAC tests were conducted according to the selected temperature requirements for the DFKI-X2D at ZARM Technik AG. To test the limits of the motor and electronics slowly, the tests started with a lower temperature range of $-30$ °C to 80 °C for the first cycles and ended with the full temperature range of $-40$ °C to 120 °C for the final cycles. Due to time constraints, only nine cycles were tested in total, with six at the lower temperature range and three at the higher temperature range. In each case, the first cycle of the different profiles started at the non-operating temperatures (TNO-max and TNO-min), which were maintained for two hours. Subsequently, the start-up temperatures (TSU-max and TSU-min) were approached, the electronics were switched on, and each temperature was maintained again for two hours. Finally, the operating temperatures (TOP-max and TOP-min) were approached, and the motor was set in motion. This was maintained for another two hours at each temperature. From this point onwards, only the TOP-max and TOP-min temperatures were switched between. Test parameters and setup are shown in Figure 3.

To simulate the load on the motor of a walking robot, a mechanical brake with an eccentric brake disc was used to generate a sinusoidal load profile. The brake was adjusted to produce a load peak at the nominal torque of 8 Nm. The motor rotated at 20 rpm, corresponding to a slow walking gait as typically observed in legged robotic platforms.

https://doi.org/10.3390/engproc2026133027

| Test parameter | Value | |
|---|---|---|
| | Run 1 | Run 2 |
| TNO-max | 80°C | 120°C |
| TSU-max | 60°C | 85°C |
| TOP-max | 50°C | 80°C |
| TOP-min | −20°C | −30°C |
| TSU-min | −25°C | −35°C |
| TNO-min | −30°C | −40°C |
| Temperature gradient | 5-10K/min | 5-10K/min |
| Hold time | 2 h | 2 h |
| Tolerance of max. hold temperatures | +3/ −0 K | +3/ −0 K |
| Tolerance of min. hold temperatures | −3/+0 K | −3/+0 K |
| Stability criterion | 1°C/h | 1°C/h |
| Vacuum | < 1*10E−5mbar | < 1*10E−5mbar |
| Cycles | 6 | 3 |

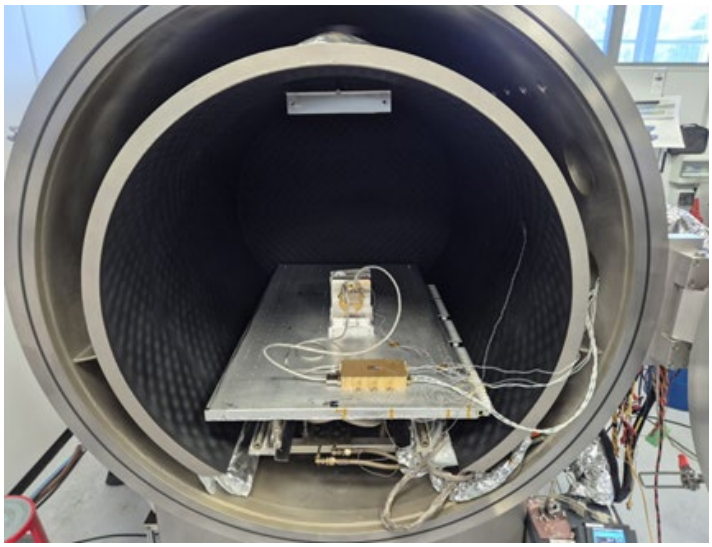


**Figure 3.** Parameters for the TVAC tests and setup in the chamber at Zarm Technik AG.

### *3.4. EMC Tests*

The EMC tests were planned and conducted at the DLR Bremen in accordance with ECSS-E-ST-20-07C [11], comprising multiple tests for the motor and electronics, including ECSS clauses 5.2.2 to 5.2.15, with exclusion of 5.2.6 and 5.2.13. The cables connected and tested were as follows: the 48 V power supply for the power segment; the 12 V power supply for the microcontroller segment; the RS422 for communication with a laptop. The following connections to the motor were also tested: a PWM signal; and a connection for reading out the encoder and sensor data. The motor was operated under load using the same brake setup as for the TVAC tests.

## 4. Results

### *4.1. Motor Characterization Results*

Figure 4 shows the characterization curve of the DFKI-X2D, and Figure 5 the heatmap with efficiency values, both of which were obtained from the tests with the commercial controller.

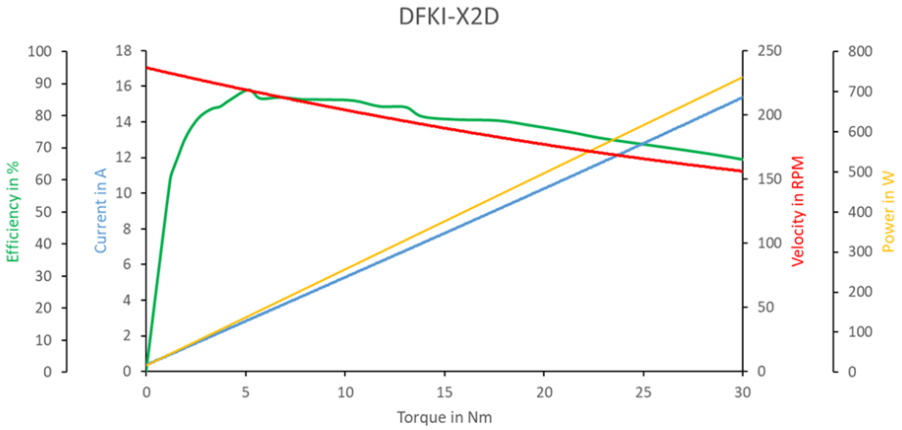



**Figure 4.** Characterization curve of the DFKI-X2D.

https://doi.org/10.3390/engproc2026133027

| Velocity in RPM | Torque in Nm | | | | | | | | | | | | | | | | | | | | | |
|---|---|---|---|---|---|---|---|---|---|---|---|---|---|---|---|---|---|---|---|---|---|---|
| | 1.3 | 1.4 | 1.6 | 1.8 | 2.2 | 2.5 | 3.1 | 3.9 | 4.4 | 5.2 | 6.0 | 7.4 | 8.7 | 10.3 | 11.5 | 13.2 | 14.7 | 15.9 | 17.5 | 19.4 | 21.5 | 24.5 |
| 16.7 | 0.58 | 0.62 | 0.72 | 0.65 | 0.66 | 0.71 | 0.76 | 0.74 | 0.70 | 0.65 | 0.62 | 0.61 | 0.62 | 0.59 | 0.54 | 0.51 | 0.48 | 0.43 | 0.41 | 0.38 | 0.36 | 0.34 |
| 33.3 | 0.71 | 0.76 | 0.82 | 0.72 | 0.79 | 0.68 | 0.79 | 0.74 | 0.75 | 0.79 | 0.73 | 0.76 | 0.73 | 0.72 | 0.67 | 0.65 | 0.63 | 0.58 | 0.55 | 0.53 | 0.51 | 0.48 |
| 50.0 | 0.81 | 0.78 | 0.82 | 0.81 | 0.74 | 0.81 | 0.74 | 0.79 | 0.85 | 0.85 | 0.77 | 0.80 | 0.79 | 0.78 | 0.74 | 0.72 | 0.71 | 0.67 | 0.64 | 0.61 | 0.59 | 0.58 |
| 66.7 | 0.74 | 0.73 | 0.80 | 0.78 | 0.84 | 0.74 | 0.80 | 0.82 | 0.83 | 0.83 | 0.79 | 0.82 | 0.82 | 0.82 | 0.78 | 0.78 | 0.77 | 0.73 | 0.70 | 0.68 | 0.66 | 0.65 |
| 83.3 | 0.72 | 0.73 | 0.76 | 0.79 | 0.84 | 0.82 | 0.88 | 0.89 | 0.84 | 0.84 | 0.82 | 0.83 | 0.83 | 0.84 | 0.80 | 0.81 | 0.80 | 0.76 | 0.73 | 0.71 | 0.69 | 0.68 |
| 100.0 | 0.66 | 0.69 | 0.71 | 0.72 | 0.79 | 0.79 | 0.84 | 0.87 | 0.85 | 0.85 | 0.83 | 0.85 | 0.85 | 0.85 | 0.82 | 0.82 | 0.82 | 0.78 | 0.75 | 0.73 | 0.71 | 0.71 |
| 116.7 | 0.66 | 0.67 | 0.71 | 0.75 | 0.79 | 0.77 | 0.82 | 0.88 | 0.86 | 0.85 | 0.84 | 0.86 | 0.86 | 0.87 | 0.84 | 0.85 | 0.84 | 0.79 | 0.78 | 0.75 | 0.74 | 0.74 |
| 133.3 | 0.63 | 0.65 | 0.71 | 0.71 | 0.76 | 0.75 | 0.80 | 0.88 | 0.86 | 0.87 | 0.85 | 0.87 | 0.87 | 0.88 | 0.85 | 0.85 | 0.85 | 0.81 | 0.79 | 0.77 | 0.76 | 0.76 |
| 150.0 | 0.57 | 0.57 | 0.63 | 0.67 | 0.74 | 0.74 | 0.79 | 0.87 | 0.85 | 0.86 | 0.85 | 0.88 | 0.87 | 0.89 | 0.86 | 0.87 | 0.86 | 0.83 | 0.81 | 0.79 | 0.78 | 0.78 |
| 166.7 | 0.59 | 0.61 | 0.62 | 0.67 | 0.72 | 0.73 | 0.80 | 0.87 | 0.86 | 0.87 | 0.86 | 0.88 | 0.89 | 0.90 | 0.87 | 0.88 | 0.87 | 0.84 | 0.82 | 0.80 | 0.79 | 0.80 |
| 183.3 | 0.63 | 0.63 | 0.66 | 0.66 | 0.72 | 0.73 | 0.79 | 0.84 | 0.84 | 0.85 | 0.85 | 0.89 | 0.89 | 0.90 | 0.88 | 0.88 | 0.88 | 0.85 | 0.83 | | | |
| 200.0 | 0.57 | 0.62 | 0.69 | 0.68 | 0.73 | 0.72 | 0.78 | 0.85 | 0.86 | 0.86 | 0.84 | 0.89 | 0.89 | 0.91 | 0.88 | | | | | | | |
| 216.7 | 0.59 | 0.66 | 0.68 | 0.67 | 0.69 | 0.71 | 0.77 | 0.83 | 0.84 | 0.85 | | | | | | | | | | | | |

**Figure 5.** Heatmap of efficiency depending on velocity and torque for the DFKI-X2D.

The tests yielded promising results for the DFKI-X2D joint. Initially, a torque of 0.3 Nm was measured in the backdrivability tests, corresponding to a 66% optimization compared to the in-runner prototype, which measured 0.9 Nm. The motor's maximum speed was 235 rpm at idle and could still reach 200 rpm within the nominal torque range. The motor demonstrated excellent efficiency, reaching approximately 90%, which corresponded to an increase of about 8% compared to the in-runner prototype (updated value of 82% for the prototype after new tests compared to [2]). The heat map showed that, within the nominal torque range of 5–10 Nm, the motor achieved high efficiency over most of the speed range, ideal for the use case example. Overall, optimizations were evident compared to the prototype, and the DFKI-X2D delivered an excellent result for a dynamic quasi-direct drive motor.

For the newly developed electronics, optimization potential was identified. At the time of testing, the maximum speed was 140 rpm, and the maximum efficiency was approximately 82%. However, it was apparent that, within the nominal torque range of 5–10 Nm, efficiency was higher than 70% or close to this level across all speed ranges. These values depend mainly on the software and control parameters, which require further testing to optimize and reach the identified potential for the DFKI-X2D. Nevertheless, the values were sufficient to proceed with the qualification tests of the motor and electronics together.

### *4.2. Vibration Tests Results*

Figure 6 displays the results of the functional tests. The graph shows an increase in power consumption in the "after vertical" curve, which represents the final direction of the vibration tests. This increase can be explained by the loosening of two screws, which was visible upon inspecting the motor. However, this did not pose a major problem because the loosening was due to insufficient glue, because at that point of time it should still be possible to carry out a subsequent non-destructive inspection of the motor. Accordingly, sufficient gluing of the screw would solve this problem, which would be planned for in actual use in a mission anyway. Contrarily, the increase in current was only approximately 0.13 A, a level which would have a negligible impact during operation under load. After retightening the screws, another measurement was taken ("after repair"), which restored the condition prior to the vibration tests and indicated that no damage had occurred.

Overall, the motor and its electronics remained fully functional and undamaged after the tests, so the vibration tests were considered a success.

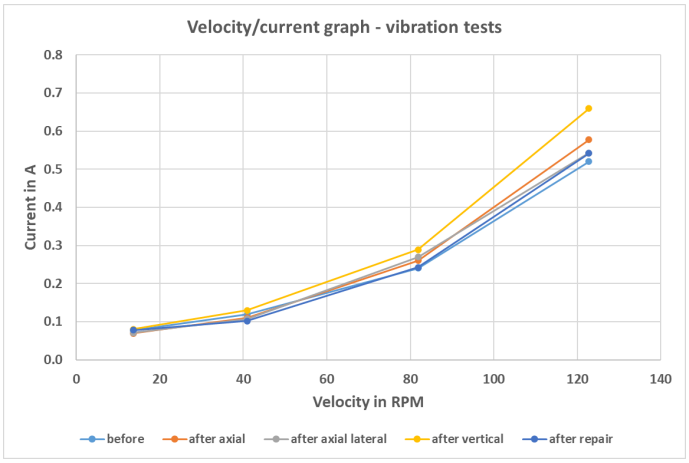



**Figure 6.** No-load current depending on velocity at different vibration test stages.

### *4.3. TVAC Tests Results*

During the cycles, various data were recorded; these included current consumption for the specified load setup, and temperatures of the motor and electronics. Figure 7 shows the average peak current consumption during the cycles and at defined phases, including before the tests, between the two temperature profiles, and after the tests. Notably, the current values were particularly high during the first cycle due to poor motor calibration caused by insufficient power usage during calibration. However, this did not pose a major problem. Although the motor heated up to 90 °C, both motor and electronics functioned without issue, proving that they remain operational even under extreme conditions. For the remaining cycles, the calibration was performed correctly, and the current values were within the expected range, with slightly higher power consumption at colder temperatures. In the first temperature profile, a drop in power consumption was observed up to the sixth cycle, a finding which can be attributed to wear on the mechanical brake. For this reason, it was preloaded again before the second temperature profile to provide the nominal torque as a load. The motor's thermal behavior was also very good during the tests. With the exception of the first cycle, the motor heated up by approximately 5 °C in most cases, and by just under 10 °C at a maximum, at temperatures of −30 °C. Because the first cycle demonstrated that the motor could withstand even higher temperatures (up to 125 °C according to the datasheet), it always operated within an acceptable range. In terms of electronics, the processor heated up by approximately 15 °C, though it always remained within a safe range. The rest of the electronics were thermally well connected and hardly heated up at all.

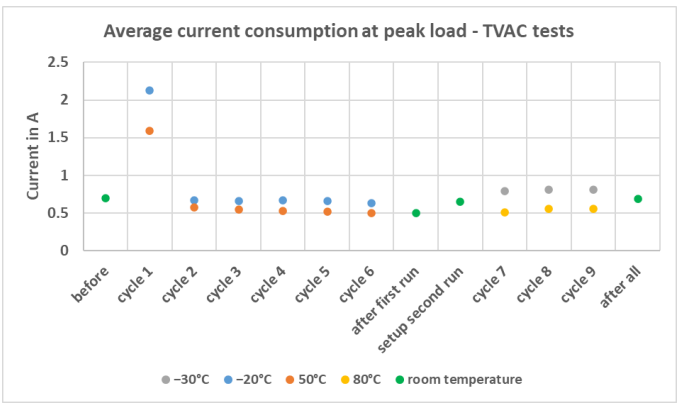



**Figure 7.** Average current consumption at peak load during the different phases of the TVAC tests at various ambient temperatures.

Overall, the TVAC tests were successfully completed. The motor and electronics could withstand extreme temperatures ranging from −30 °C to 120 °C, remaining fully functional throughout all cycles and after the tests.

### *4.4. EMC Tests Results*

Three of the tests performed could not be passed, including conducted emission at 100 kHz to 100 MHz, inrush currents, and conducted susceptibility at 30 Hz to 100 kHz. It was apparent that the problems occurred in the 48 V line of the electronics in all these tests. During the tests, initial conclusions about possible causes of errors and necessary adjustments to the electronics could already be drawn based on the frequencies and the error cases. The remaining tests, as well as the other lines in the same tests, were passed. There were no problems whatsoever with the motor or the general shielding. Overall, this meant that the EMC tests were only partially successful.

## 5. Conclusions and Outlook

Overall, the DFKI-X2D joint performed consistently well in all tests. The functional tests confirmed its excellent efficiency and dynamics. In the environmental tests, the motor successfully completed all tests and remained fully functional. The motor completed over 100,000 revolutions on the output side, approximately 50,000 of which were performed under the extreme conditions of the TVAC tests. This is equivalent to approximately 50 km of running distance for a dynamic walking robot, and it served as additional long-term testing. These results lead to an increase to TRL 5 for the DFKI-X2D.

The electronics also performed well in the tests, although, in comparison with the motor, there is still room for improvement. Except for the three EMC tests, the electronics passed all environmental tests without issue, demonstrating excellent thermal behavior and a robust design. Overall, the electronics achieved a TRL 4, because the EMC tests were partially failed and radiation tests were left out at this stage.

Looking to the future, there is still room for improvement. The motor's scalability could be highlighted, and protection against harsh lunar dust could be added. The electronics could be downsized and integrated into the motor design to create a single unit. There is also the goal of raising the TRL level for both, as the achievement of a space-ready design draws closer. Additionally, other use cases for the DFKI-X2D can be considered, such as dynamic manipulator arms; or use in different tools, like in the application area of the EU RISE (European Robotics for Space Ecosystems) project [12]. Overall, further research is required to apply the DFKI-X2D joint to future missions. This means that appropriate robotic systems must be developed.

**Author Contributions:** Writing, J.E. and W.B.; testing, J.E. and Z.Z. and P.W.; design, J.E. and Z.Z. and P.W. All authors have read and agreed to the published version of the manuscript.

**Funding:** This research was funded by the Federal Ministry for Economic Affairs and Climate Action, as well as the German Aerospace Center (DLR), grant numbers 50RA2107 and 50RA2108. Funding was also received from the European Union's Horizon Research and Innovation Program under grant agreement No 101134934. Partially supported by the German Federal Ministry of Research, Technology and Space (BMFTR) under the Robotics Institute Germany (RIG).

**Institutional Review Board Statement:** Not applicable.

**Informed Consent Statement:** Not applicable.

**Data Availability Statement:** Data is contained within the paper.

**Conflicts of Interest:** The authors declare no conflicts of interest. The funders had no role in the design of this study; in the collection, analyses, or interpretation of data; in the writing of the manuscript; or in the decision to publish the results.

## References

1. Brinkmann, W.; Schilling, M.; Chowdhury, P.; Eisenmenger, J.; Benz, J.; Langosz, M.; Li, J.; Michelson, E.; Yüksel, M.; Kirchner, F. Toward Sustainable Space Exploration: Designing an AI-Powered Modular Toolbox for Future Planetary Exploration. *Eng. Proc.* **2025**, *90*, 26. [CrossRef]
2. Eisenmenger, J.; Zhao, Z.; Kirchner, F. Development of Quasi-Direct Drive Motor for Walking Robots in Extraterrestrial Environments. *Eng. Proc.* **2025**, *90*, 99. [CrossRef]
3. Katz, B.; Carlo, J.; Kim, S. Mini Cheetah: A Platform for Pushing the Limits of Dynamic Quadruped Control. In Proceedings of the 2019 International Conference on Robotics and Automation (ICRA), Montreal, QC, Canada, 20–24 May 2019; pp. 6295–6301.
4. Unitree. Available online: https://www.unitree.com/a1/ (accessed on 4 November 2025).
5. Valsecchi, G.; Weibel, C.; Kolvenbach, H.; Hutter, M. Towards Legged Locomotion on Steep Planetary Terrain. In Proceedings of the 2023 IEEE/RSJ International Conference on Intelligent Robots and Systems (IROS), Detroit, MI, USA, 1–5 October 2023; pp. 786–792.
6. Miki, T.; Lee, J.; Hwangbo, J.; Wellhausen, L.; Koltun, V.; Hutter, M. Learning robust perceptive locomotion for quadrupedal robots in the wild. *Sci. Robot.* **2022**, *7*, eabk2822. [CrossRef] [PubMed]
7. Valsecchi, G.; Liconti, D.; Tischhauser, F.; Kolvenbach, H.; Hutter, M. Preliminary design of actuators for walking robot on the moon. In *16th Symposium on Advanced Space Technologies in Robotics and Automation (ASTRA 2022)*; ETH Zurich, Institute of Robotics and Intelligent Systems: Zürich, Switzerland, 2022.
8. Williams, J.-P.; Paige, D.; Greenhagen, B.; Sefton-Nash, E. The global surface temperatures of the Moon as measured by the Diviner Lunar Radiometer Experiment. *Icarus* **2017**, *283*, 300–325. [CrossRef]
9. Henninger, J.H. *Solar Absorptance and Thermal Emittance of Some Common Spacecraft Thermal-Control Coating*; NASA: Washington, DC, USA, 1984.
10. *ECSS-E-HB-32-26A*; Space Engineering: Spacecraft Mechanical Loads Analysis Handbook. European Cooperation for Space Standardization: Noordwijk, The Netherlands, 2013.
11. *ECSS-E-ST-20-07C Rev.2*; Electromagnetic Compatibility. European Cooperation for Space Standardization: Noordwijk, The Netherlands, 2022.
12. Eisenmenger, J.; Diaz-Carrasco, M.; Manz, M.; Vinals, J. Development and application of Interchangeable Tools for Modular In-Orbit Assembly Scenarios. In Proceedings of the 76th International Astronautical Congress (IAC 2025), Sydney, Australia, 29 September–3 October 2025. [CrossRef]

**Disclaimer/Publisher's Note:** The statements, opinions and data contained in all publications are solely those of the individual author(s) and contributor(s) and not of MDPI and/or the editor(s). MDPI and/or the editor(s) disclaim responsibility for any injury to people or property resulting from any ideas, methods, instructions or products referred to in the content.